Local multiplicity fluctuations as a signature of critical hadronization in heavy-ion collisions at TeV energies

Rudolph C. Hwa[1] and C. B. Yang[1,2]
[1]*Institute of Theoretical Science and Department of Physics University of Oregon, Eugene, Oregon 97403-5203, USA*
[2]*Institute of Particle Physics, Central China Normal University, Wuhan 430079, People's Republic of China*
(Received 5 December 2011; revised manuscript received 17 January 2012; published 13 April 2012; corrected 27 April 2012)

In central Pb-Pb collisions at the Large Hadron Collider the multiplicity of particles produced is so high that it should become feasible to examine the nature of transition from the deconfined quark-gluon state to the confined hadron state by methods that rely on the availability of high-multiplicity events. We consider four classes of the transition process ranging from critical behavior to totally random behavior, depending on whether there is clustering of quarks and whether there is contraction of dense clusters owing to confinement. Fluctuations of bin multiplicities in each event are quantified, and then the event-by-event fluctuations of spatial patterns are analyzed. A sequence of measures is proposed and is shown to be effective in capturing the essence of the differences among the classes of simulated events. It is demonstrated that a specific index has a low value for critical transition but a larger value if the hadronization process is random.

DOI: 10.1103/PhysRevC.85.044914 PACS number(s): 24.60.Ky, 25.75.Nq

I. INTRODUCTION

Phase transition has always been a subject of great interest in many fields. The possibility of observing evidences for the critical point in heavy-ion collisions has invigorated extensive experimental programs at various laboratories [1,2]. At the Large Hadron Collider (LHC), where the collision energy is much higher, the physics of hadronization involves issues that are different from that probed at lower energies where high chemical potential is expected. Because a hot and dense plasma is produced at LHC, the deconfined state persists for a long time before the system is dilute enough to undergo transition to the hadron phase. That transition may or may not be recognizable as a critical phenomenon because hadronization takes place on the surface over a period of time while the system expands. The accumulation of hadrons emitted over that period can smear out any signal of interest even in the best circumstance for critical transition, which is not assured on theoretical grounds. It is therefore a challenge to discover from the data collected at LHC phenomenological features that can reveal the nature of the transition from quarks to hadrons. Our aim in this work is to find the most effective way to extract dynamical signals indicative of the collective behavior the quark-gluon plasma (QGP) making that transition. Our search does not rely on the validity of any theoretical view on the possibility of critical behavior in heavy-ion collisions at very high energy.

A large amount of data on Pb-Pb collisions at LHC has been produced in the past year [3]. Compared to earlier expectations [4] by extrapolation from the Relativistic Heavy-Ion Collider (RHIC) some significant differences have been found. For example, the pseudorapidity density $(dN_{\rm ch}/d\eta)(N_{\rm part}/2)$ at midrapidity has been predicted in Ref. [5] to be around 6 in central collisions at LHC by extrapolation from RHIC and lower energies, whereas the actual data turn out to be 8–9 [6–8]. The nuclear modification factor R_{AA} is found to have a strong rise for $p_T > 7$ GeV/c, which is generally expected from energy loss models [4,9]. For such predictions to be made by extrapolation from lower energies, it is necessary to have the measureable quantities to be already determined at those energies. We raise the question whether there are observables to be measured at LHC that have not been feasible for analysis at RHIC, so there would be no basis from which to extrapolate.

An obviously outstanding feature of the data obtained at LHC is that the total multiplicity $N_{\rm ch}$ of charged particles produced is unprecedentedly high, around 6×10^3 in central collisions at 2.76 TeV [6]. Observables that rely on large $N_{\rm ch}$ can thus be exploited in ways that could not have been possible at lower energies, thereby forming a frontier that has not been explored. Another aspect of central Pb-Pb collisions is that there is surely a deconfined system of quarks and gluons, which must undergo some kind of transition to the confined state of hadrons. Theoretically, the use of the Cooper-Frye scheme [10] to calculate the hadronic properties avoids the issue about the nature of the deconfinement-to-confinement transition. There are three aspects about the QGP: birth, life, and death. The traditional approach to relating the properties of QGP to observables is to use hydrodynamics (on the fluid flow) to describe the life and the Cooper-Frye scheme for its death (based on local conservation laws at freeze-out surface without reference to quarks), so that specific birth configurations can lead to calculable results that can be compared to global data. Studies of QCD phase transition (PT) have thus far been more concerned with the birth problem than the death problem. That is why beam energy scan has been proposed at low energies where one hopes to create a system near the critical point at the end of the phase boundary between quark and hadron phases [11]. Our concern here is the opposite. We focus only on the death problem of the quark-gluon system which is created at as high an energy as possible and lives for a long time; it is when it dies that the transition to hadrons leaves the footprint which we try to find. We leave open the question of what the nature of that transition is. We propose four scenarios that range from critical behavior on one end to noncritical on the other, and investigate whether the proposed measures can

possibly distinguish those cases. We simulate the events in each case and examine the effectiveness of the measures.

The theme of our investigation is about the fluctuations of spatial patterns during the quark-hadron transition. The momentum of each particle is usually expressed in terms of (p_T, η, ϕ), where p_T is the transverse momentum, η the pseudorapidity, and ϕ the azimuthal angle. For any interval of p_T one can study the (η, ϕ) distribution in any given event, called the lego plot, when shown in some finite-size binning. For convenience, we refer to that distribution as a spatial pattern, which changes from event to event. The basic question is whether the fluctuations of those patterns contain any information about the nature of the quark-hadron transition. To study those patterns one needs good resolution from the experimental side and efficient description from the theoretical side. Furthermore, one should not integrate over all p_T because the superposition of different patterns at different Δp_T intervals can smear out all recognizable features. Thus, to be able to have high resolution in all (p_T, η, ϕ) variables as well as to have enough particles in small bins in each variable requires high event multiplicities. That is where the LHC data become extremely useful.

There are recent reports from ALICE on the event-by-event fluctuations of global observables in Pb-Pb collisions [12,13]. Nonstatistical fluctuations of mean p_T are found to be lower than a scaling behavior in event multiplicity as the collisions become more central. For those central collisions the data on p_T fluctuations have recently been explained in a study of the effect of initial-state fluctuation on the p_T correlation in the framework of color glass condensate [14]. The success of that line of investigation on the birth problem does not render meaningless our inquiry into the unexplored question about the death problem. In particular, it is still unknown what the nature of the transition is from quarks to hadrons.

There are two kinds of fluctuations that we consider. One is the fluctuation of bin multiplicity from bin to bin in an event, and the other is the event-to-event fluctuation of the spatial patterns. On the former it can be just random fluctuations, but it can also be in the form of clusters of all sizes, as in second-order PT [15]. Both types of patterns will be generated to initiate quark configurations in the (η, ϕ) space before and during time evolution throughout the period of hadronization for two distinct classes of models. Hydrodynamical flow during the life of QGP does not dictate the nature of the quark configurations because it describes the macroscopic fluid properties. We construct an algorithm for simulating the effect of color confinement through contractions of dense clusters between time steps in the hadronization period and the opposite effect of thermal agitation by randomization right after each contraction. Pion formation according to chosen criteria can occur throughout the process, resulting in an event distribution of pions in (p_T, η, ϕ). That distribution is then analyzed by factorial moments to filter out statistical fluctuations. Repeating the simulation over many times generates event-by-event fluctuations which turn out to be crucial to the finding of revealing signatures. Large deviations from the average event structure are possible but very rare; however, they can make significant influence on the measure that we propose.

We recall that the use of factorial moments (FMs) in the study of hadronic multiplicity fluctuations has been referred to as intermittency [16]. During the quarter century since its initial proposal a great deal of effort has been given to the subject of learning about dynamical fluctuations of the multiparticle system and to further expansion beyond intermittency [17]. A large body of experimental results from the analyses of data on nuclear collisions using FMs has been obtained for various collisional systems at various energies, as described in Ref. [17] and beyond [18–25]. However, at RHIC energies and lower, the total multiplicities are not high enough to avoid substantial averaging that erases some aspects of the fluctuations. At LHC the much higher multiplicities make possible more detailed studies of local properties in (η, ϕ) for narrow bins of p_T in each event. What we do here goes far beyond earlier studies because (a) the quark system before hadronization can be generated to simulate critical behavior as has never been done before, (b) time evolution during the hadronization period can be designed to take into account possible contraction owing to collective confinement forces, and (c) event-by-event fluctuations are investigated by studying the moments of moments, made feasible by high multiplicities at LHC. Thus, we emphasize that neither our theoretical consideration in this paper nor the recommended experimental investigation should be regarded as a simple extension of the original intermittency idea to LHC energy.

The outline of this paper is as follows. In Sec. II we first give a quick review of FM and then describe how a configuration of quarks (not hadrons) can be generated to possess the properties of a system entering into a second-order PT using the FM as a measure. Section III contains the physics issues that are to be addressed concerning the various possibilities that a quark system would behave as its density becomes low enough for hadronization, that is, with or without clustering and with or without contraction. Procedures for simulating the various scenarios are given. In Sec. IV we define the moments of moments to quantify the event-by-event fluctuations of the spatial patterns to be used in the section that follows; they are basically a review of earlier studies. We then describe in detail the results of our calculations for the various hadronization schemes in Sec. V. They give a framework to interpret the results of future analyses of the actual data collected at LHC. Section VI contains the conclusion of this work.

II. LOCAL MULTIPLICITY FLUCTUATIONS WITH CRITICAL CLUSTERING

In searching for ways to simulate configurations that have a wide range of characteristics without theoretical prejudices, ranging from critical to noncritical cases, we focus in this section on finding a simple procedure to generate configurations that correspond to critical behavior. We first review a number of related investigations on the local behaviors of multiplicity fluctuations of systems undergoing a second-order PT describable by the Ginzburg-Landau (GL) theory. They are then to be connected to a distribution of cluster production that can readily be used to simulate initial configurations before hadronization begins. Only one parameter is needed to describe

the clustering. Later, for the noncritical case it is only necessary to change that parameter so as to obtain random distributions.

It was suggested that the normalized FMs F_q can be used as a quantitative measure of local fluctuations [16]. F_q is defined by

$$F_q(\delta) = \frac{\langle n!/(n-q)!\rangle}{\langle n\rangle^q}, \tag{1}$$

where n is the multiplicity in a bin of size δ^d in a d-dimensional phase space, and the averages are performed over many events. A power-law behavior,

$$F_q(\delta) \propto \delta^{-\varphi_q}, \tag{2}$$

over a range of small δ is referred to as intermittency and has been observed in many systems of collisions [17]. The virtue of F_q is that it filters out statistical fluctuations, as can be seen as follows. If the multiplicity distribution P_n can be written as a convolution of the Poisson distribution $P^0_{\bar{n}}(n)$ and a dynamical distribution $D(m)$, that is,

$$P_n = \int_0^\infty dm \frac{m^n}{n!} e^{-m} D(m), \tag{3}$$

then the numerator of F_q is

$$\sum_{n=q}^{\infty} \frac{n!}{(n-q)!} P_n = \int_0^\infty dm m^q D(m), \tag{4}$$

which is a simple moment of $D(m)$. Thus, if the dynamics is trivial, that is, $D(m) = \delta(m - \bar{n})$, then $F_q = 1$ for all q. Any deviation from 1 is then a measure of nontrivial dynamical fluctuations, and a power-law behavior in Eq. (2) would suggest a dynamics that is not characterized by a particular scale [16]. The footprint of a PT that has fluctuations of all scales may then be possibly observed in the measurement of intermittency [26].

To obtain a theoretical quantification of PT in terms of F_q, a study of second-order PT in the GL theory was carried out in Ref. [27], in which the order parameter is identified with the multiplicity density. It is found that to a high degree of accuracy F_q satisfies the power-law behavior

$$F_q \propto F_2^{\beta_q}, \tag{5}$$

where

$$\beta_q = (q-1)^\nu, \quad \nu = 1.304, \tag{6}$$

essentially independent of the details of the GL parameters. Such a behavior was experimentally verified by the study of photon number fluctuations of a single-mode laser at the threshold of lasing [28], confirming that it is a PT problem describable by GL theory [29]. On the theoretical side, it has also been found that using the 2D Ising model to simulate quark-hadron PT the resulting scaling behavior of F_q is in agreement with Eqs. (5) and (6) [30]. It does not mean, however, that an analysis for F_q in the current data from heavy-ion collisions can verify or falsify the connection between hadronization and second-order PT because of the complications that are present in such systems but absent in the optical system. The following sections are aimed at addressing such complications. We note that in the discussion above concerning Eqs. (1) to (6) no mention is made of the specifics about multiplicities, whether hadrons or quarks. In the remainder of this section we use particles as a generic term that can refer to either hadrons or quarks. The result obtained is used in the following sections to generate configurations of quarks (and/or antiquarks) just before hadronization.

From a different perspective it is of interest to study the problem of clustering, because the critical phenomenon is known to be characterized by clusters of all sizes. It is a subject relevant to our investigation here because we analyze the two-dimensional (2D) spatial distribution of particles in the η-ϕ space. Cluster formation in the context of hadronization has been considered before [31], but from the point of view of self-organized criticality instead of second-order PT. Because the latter exhibits the behavior of Eqs. (5) and (6), it is not difficult to see how such a behavior can be achieved by an adjustment of the scaling property of the cluster formation.

As a generic problem on clusters of particles, let C be the number of particles in a cluster, and $P(C)$ be the probability distribution in C, which we assume to have the scaling form

$$P(C) \propto C^{-\gamma}, \quad \gamma > 0. \tag{7}$$

We let the center of a cluster be distributed randomly in a 2D space which we take to be 1 unit of length on each side. We further let a particle in a cluster C be distributed randomly around its center with a Gaussian width of

$$\sigma = 0.1\, C^{-1/2}, \tag{8}$$

so that there can be high density of particles, though with decreasing probability at high C. Such spikes of multiplicity are what can give rise to intermittency.

To investigate the multiplicity fluctuations in small bin sizes, we divide the unit square into $M \times M$ bins, M varying from 8 to 70. We let N_0 particles be distributed in the unit square in accordance with Eqs. (7) and (8) and allow N_0 to be approximately 100, because the sum of all clusters may not be exactly the same for every event. With n being the number of particles in a bin, we perform the calculation for $F_q(\delta)$ according to Eq. (1), by averaging over all bins first, and then averaging over all (5×10^5) events for any fixed $\delta = 1/M$. Only bin multiplicities with $n \geqslant q$ are counted in $F_q(M)$. The result for $\gamma = 2$ is shown in Fig. 1(a), which exhibits nontrivial dependence on M; it is not strictly linear in the log-log plot. However, when F_q is plotted against F_2 for $q = 3, 4, 5$, very good linearity is found, as shown in Fig. 1(b) replicating the behavior found for GL [27]. Similar power-law behavior is obtained for other values of γ. We show in Fig. 1(c) the dependence of the exponent β_q, defined in Eq. (5), on $q - 1$ and find in accordance with Eq. (6) that $\nu = 1.136$, 1.171, and 1.315, for $\gamma = 1.5$, 2.0, and 2.5, respectively.

What we have done above is to find a quick way to relate a particle distribution in a 2D space to a GL-type F_q-scaling behavior through the use of a cluster distribution. Because a range of values of ν has been obtained, the relationship between γ and ν has no specific dynamical significance. It merely demonstrates that large local multiplicity fluctuations can generate large F_q with scaling properties. In the case of $\gamma = 2.5$ we see in Fig. 1(c) that the straight line connecting the three points, when extrapolated to $q = 1$, does not go through

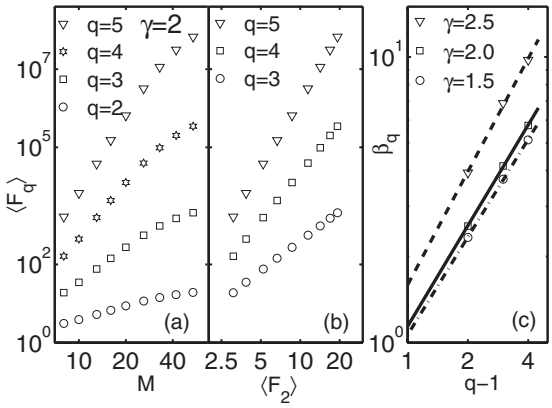

FIG. 1. Intermittency analysis of clustering model for $\gamma = 2$ in Eq. (7): (a) scaling in M, (b) F scaling in F_q vs F_2, and (c) power-law behavior of β_q in Eq. (6).

$\beta_2 = 1$, thus showing slight deviation from Eq. (6). The special value $\nu = 1.3$ for second-order PT can approximately be achieved by using a value of γ between 2.0 and 2.5. Although no dynamics has been introduced to establish that connection, our objective here is accomplished by having found a simple procedure to simulate configurations that may be relevant to a quark and antiquark system that is at the edge of PT to hadrons. This is only the starting point of a much more complicated problem in heavy-ion collisions that we describe next.

III. SIMULATION OF EVENTS WITH SPATIAL FLUCTUATIONS IN HEAVY-ION COLLISIONS

If there is no dynamical structure in the spatial pattern of soft hadrons in the lego plot (of η and ϕ), then there should be nothing interesting in whatever measure that is used to analyze the data. The reverse is, however, not necessarily true. Unless a measure is sensitive to the consequence of certain dynamics, one may not observe what is interesting. To provide motivation for an experimental effort to search for an unconventional signal, it is necessary to demonstrate the worthiness of such an effort under the best of circumstances. The optimal scenario is that the quark-gluon system undergoes a second-order PT in forming hadrons so that there are large multiplicity fluctuations. It is not known whether such a phenomenon occurs at LHC. Our aim here is to simulate events that belong to different classes of dynamical characteristics, ranging from robust criticality to mundane randomness. For each class of hadronization the measure to be used in the following section should exhibit distinguishing features in the hope that analysts of the real data would have the incentive to pursue the more difficult task of extracting worthwhile information from what is actually observed.

The physics we aim to simulate is for the duration between the end of the quark phase and the beginning of the hadron phase. It is assumed that the density is so low that the confining forces among the quarks and the antiquarks begin to redistribute them spatially. Gluons are assumed to have been converted to q and $\bar{q}$ that are the basic units prior to hadronization. We restrict our attention to the central rapidity region with $|\eta| \leqslant 1$ and $0 \leqslant \phi \leqslant 2\pi$ for central collisions. The surface of the plasma cylinder with those values of η and ϕ is mapped to the unit square S. Because the fluctuation properties to be discussed below do not depend on the precise area that S corresponds to, a portion of the (η, ϕ) region in the actual data should suffice to serve as a workable basis for analysis. The cylinder hadronizes at the surface only, layer by layer. Thus, we have to consider many time steps $t_i, i = 1, 2, \ldots$. Between adjacent time steps the q and $\bar{q}$ adjust their positions in S in accordance to a procedure that we impose to simulate confinement and pion emission. The quarks have thermal p_T distribution whose inverse slope T_i decreases incrementally with t_i. At a new time step a new set of q and $\bar{q}$ are introduced to represent the movement of the next layer of quarks to the surface. The confinement procedure starts over again until most of the quarks (not necessarily all) are pionized before another time step is taken. This is a general outline of the algorithm to convert q and $\bar{q}$ to pions, whose coordinates in (p_T, η, ϕ) are registered for event-by-event analysis later.

The main part of our physics input is the deconfinement to confinement transition between time steps. The principal characteristic of a critical phenomenon is the tension between the ordered and the disordered motions of a system. In the Ising model of a magnetic system the near-neighbor interaction between spins tends to align all spins in the same direction, but the thermal motion tends to randomize them. If the quark-hadron PT is in the same class of criticality, then the tension is between confinement that draws the $q\bar{q}$ into an ordered pair and the disordered thermal agitation that tends to keep the quark system in the deconfined state. On the surface of the plasma cylinder the q and $\bar{q}$ may start to cluster as the density and temperature get close to the transition point, thereupon a local region of high density contracts under the confinement force to improve the likelihood of a $q\bar{q}$ pair to fall within a confinement distance. In principle, we should keep track of the colors of the quarks, but that would complicate the procedure much more. The simple algorithm we adopt mimics the general idea of color confinement and generates large multiplicity fluctuations. One of the chief objectives of this work is to see whether many such local fluctuations at different time steps can survive the superposition at the end of the hadronization process, and still be detected by an effective measure. The feasibility issue is addressed at the cost of precision in QCD, which is difficult in the soft regime over an extended period.

Let us describe first the case of critical hadronization, followed later by other cases that are less critical.

A. Critical

1. Initial configuration

We start by seeding the unit square S with 500 pairs of $q\bar{q}$. They are clustered according to the probability distribution $P(C)$, given in Eq. (7). That is, C pairs of $q\bar{q}$ are placed in a cluster centered at a random point in S; they are Gaussian distributed around the center with a width specified by Eq. (8). As a result of the study in Sec. II that relates the exponents γ and ν, we choose $\gamma = 2$, corresponding to ν not quite up to 1.3. As the cluster multiplicity C is summed over all clusters,

we stop the seeding process when the total just exceeds 500. Inside each cluster the q and $\bar{q}$ are not correlated; they are independently distributed in (η, ϕ) as well as in p_T, for which the thermal distribution is the exponential, $\exp(-p_T/T)$, with T set at 0.4 GeV.

The above procedure is for setting up an initial configuration at $t_0 = 0$, counting from just before the first pions are emitted, but long after the collision time. The value of T is not set at T_c which is lower, but at a value above the observed average $\langle p_T \rangle$, because the bulk of the pions will be produced at later time when T will be lower. The clustering is put in to generate a spatial configuration that is most likely to represent a system moving toward a critical transition.

2. Pionization

In the above configuration if a q and $\bar{q}$ are within a distance d from each other that is less than $d_0 = 0.03$, then we regard the pair as effectively a pion and let it be taken away from the configuration, but registering the pion position in a separate (η, ϕ) space at the midpoint between the pair. We assign a value of p_T to that pion that is equal to the sum of the p_{iT} values of the q and $\bar{q}$. This is based on the recombination model, where the recombination function has a momentum-conserving δ function: $\delta(p_T - p_{1T} - p_{2T})$ [32–34]. The thermal distributions of quarks and pions have the same T. We ignore the color and flavor of the quarks without losing the essence of local fluctuation, because if the q and $\bar{q}$ had color and flavor labels, it would take longer in the iteration process for the $q\bar{q}$ pair in a cluster to pionize without changing the (η, ϕ) coordinates appreciably.

3. Contraction

The probability that a $q\bar{q}$ pair is within d_0 apart is small, so the majority of the quarks remain in S. They are under the influence of the color forces to move toward confinement. To describe that movement in a collective way rather than in terms of pairwise interaction that is unrealistic, we adopt the contraction procedure as follows.

Let S be divided into 5×5 bins. Calculate the number of q and $\bar{q}$ in each bin. Separate the bins into two types: Dense bins have more q and $\bar{q}$ than the average bin multiplicity, and the dilute bins have less. The difference between q and $\bar{q}$ is ignored here. If adjacent dense bins share a common side, they are grouped together as members of a cluster of dense bins. Let D refer to such a cluster of dense bins, which may have an irregular shape, but are connected. Let N_D denote the number of bins in D. Define $\vec{r}_D$ to be the coordinates in S that is the center of mass of D. Now, we do a contraction of D. That is, we redistribute all the q and $\bar{q}$ in D, centered at $\vec{r}_D$, but with a Gaussian width

$$\sigma_D = \sigma_1 N_D^{1/2}, \tag{9}$$

where σ_1 is a parameter that characterizes the degree of contraction. We use $\sigma_1 = 0.1$ here with other possibilities to be discussed later. Because of the Gaussian distribution, the q and $\bar{q}$ that are spread out originally in N_D bins are drawn closer together to be located mostly within the Gaussian peak, resulting in a contraction. Because there are 5×5 bins, the original bin size is 0.2×0.2, to which σ_D should be compared after contraction. This is how we model the effect of the ordered motion owing to confinement. We repeat step 2 to allow $q\bar{q}$ pairs to pionize in this new configuration.

4. Randomization

The disordered motion that counterbalances the ordered motion is the thermal randomization. We model that by requiring all the q and $\bar{q}$ in the dilute bins to be redistributed randomly throughout S, resulting in a new configuration. We then repeat step 3 to have another round of contraction and pionization. Each time in the iteration process more $q\bar{q}$ pairs are converted to pions, as we alternate contraction and randomization until around 95% of the $q\bar{q}$ system is depleted. We regard that as the end of one time step in which the quarks on the cylinder surface are hadronized. We then proceed to the next time step when a new layer of quarks moves up to the surface.

We note that before the next time step is taken, pionization becomes increasingly difficult when fewer and fewer q and $\bar{q}$ remain to find their partners to coalesce. Decreasing σ_1 to 0.05 speeds up the process near the end, but does not change the pion distribution in (η, ϕ) very much. Physically, it is not necessary that all $q\bar{q}$ in a layer hadronize before the next layer of quarks moves up. Leaving roughly 5% to be mixed with the next layer of $q\bar{q}$ seems reasonable in our attempt to model a continuous process of hadronization by discrete steps.

5. Subsequent time steps

To advance to the next time step we introduce 100 new pairs of $q\bar{q}$ according to the distribution $P(C)$ and add them to the existing q and $\bar{q}$ that remain from the previous step. We then follow the same procedure as above to contract, pionize, and randomize repeatedly until 5% of q and $\bar{q}$ remains. At the ith time step all q and $\bar{q}$ have the p_T distribution with an inverse slope

$$T_i = T_{i-1} - 0.02 \text{ GeV}. \tag{10}$$

That is the T_i that the pions emitted at t_i will also have. This is carried out ten times so that, in total, we introduce 1500 $q\bar{q}$ pairs, most of which turn into pions. To have approximately 1400 pions produced in $|\eta| < 1$ in central collision at LHC is not unrealistic. Because we are not interested in global multiplicity fluctuations in this study, we stop after ten steps. The pions collected in (p_T, η, ϕ) for the event is then stored for later analysis of local fluctuations.

B. Quasicritical

Consider now the case where clustering occurs neither in the initial configuration nor when new layers of q and $\bar{q}$ move to the surface. Thus, the initial 500 pairs of $q\bar{q}$ are seeded randomly in S, and so are the subsequent 100 pairs at each

time step. There is then no correspondence with the second-order PT discussed in Sec. II. Technically, this corresponds to the exponent γ in Eq. (7) being very large, because the probability for having a large cluster C is then very small. Specifically, we choose $\gamma = 5$ for no clustering. One may regard this case as being in correspondence to a crossover in the phase diagram where no distinct boundary between the quark and hadron phases can be identified. However, we require that the confinement forces to be still at work to turn quarks to hadrons. So we use the contraction-randomization procedure described in Sec. III A to carry out pionization. Such a procedure simulates the tension between confinement and deconfinement, but cannot be regarded as what is needed for a critical transition. The coordinates of each pion in (p_T, η, ϕ) are recorded as before for later analysis.

C. Pseudocritical

Suppose now that we seed the configurations with clustering, but do not impose contraction between time steps. Thus, the q and $\bar{q}$ configurations, as each layer reaches the surface, are close to the critical condition, when we set $\gamma = 2$ as we have done above. However, the hadronization process is carried out by letting $q\bar{q}$ pairs form pions whenever a pair gets close together. Without contraction we cannot require the distance between pairs to be less than d_0 as in Sec. III A 2, because the probability for that to occur is low. Without new dynamics during hadronization we simply let each quark to search for the nearest antiquark within a distance $d = 0.1$ and let a pion be formed at the position midpoint between the $q\bar{q}$ pair. Then we go to another quark and repeat the process. When no more pairs can be found within that distance, we proceed to the next time step whatever numbers of q and $\bar{q}$ are left. With more $q\bar{q}$ pairs supplied from the next layer, the probability of pionization is increased. This process will not convert all $q\bar{q}$ pairs to pions because the quarks can be far apart from antiquarks without contraction. To have quarks left over at the end of ten time steps does not matter as far as the local multiplicity fluctuation is concerned. We see that there is still interesting structure that can be extracted from the accumulated events simulated that way.

D. Noncritical

To the other extreme situation away from the above three cases we consider the noncritical case of no organized dynamics at all, that is, random configurations and no contraction. The result should not have any content of interest. We have nevertheless carried out the simulation and show the result that is nontrivial and therefore instructive. A summary of the four cases can be expressed as a matrix shown in Table I.

TABLE I. Matrix of cases of criticality.

	Clustering	No clustering
Contraction	Critical	Quasicritical
No contraction	Pseudocritical	Noncritical

IV. MOMENTS FOR EVENT-BY-EVENT FLUCTUATIONS

We now consider the method of analysis of the many events either as measured at LHC or as generated in the models described in the preceding section. Because of the high multiplicity of particles produced in central collisions, we make cuts in p_T, such as in an internal Δp_T around $p_T = 1$ GeV/c. We have considered $\Delta p_T = 0.04, 0.07$, and 0.1 GeV/c. In such small intervals the particle multiplicities are significantly reduced and spatial patterns in (η, ϕ) begin to appear because of the possibility of empty bins.

To find an effective measure of the fluctuations we need it to be sensitive to both the spatial variations from bin to bin and the event-by-event fluctuations. We refer to the former as horizontal and the latter as vertical. Different moments are to be taken for horizontal and vertical averages so as to allow spatial and eventwise fluctuations to manifest separately.

We divide the unit square into M^2 bins with M being not more than 70, depending on the multiplicity in the Δp_T interval, just so that the important part of the M dependence is captured. For the spatial fluctuations we use the horizontal FMs for event e, defined as

$$F_q^e(M) = f_q^e(M)/\left[f_1^e(M)\right]^q, \tag{11}$$

where

$$f_q^e(M) = \langle n(n-1)\cdots(n-q+1)\rangle_h. \tag{12}$$

The average $\langle\cdots\rangle_h$ is performed over all M^2 bins, n being the multiplicity in a bin. Only $n \geqslant q$ is counted in $f_q^e(M)$. Clearly, if M is very large, $f_q^e(M)$ may be zero, for $q \geqslant 2$, although $f_1^e(M)$ is never zero. However, there may be an event where $F_q^e(M)$ may not vanish at a large M; then it would imply sharp spikes of multiplicity in some bins. If the fluctuations among the bins are Poissonian, then we have $F_q^e(M) = 1$ for any M, as is the case with vertical fluctuations discussed in Sec. II. Interesting spatial fluctuations are, however, not Poissonian.

For each event we can calculate $F_q^e(M)$. We note that $F_q^e(M)$ is a simple characterization of spatial pattern, but is not the only one possible. Any alternative description can also be used in the study below on event-by-event fluctuations. One may therefore regard $F_q(M)$ as a generic symbol.

If $\langle F_q(M)\rangle_v$ denotes the vertical average of $F_q^e(M)$ over all events, then the fluctuation of $F_q^e(M)$ from $\langle F_q(M)\rangle_v$ is what we want to quantify. To that end we consider the pth-order moments of

$$\Phi_q(M) = F_q^e(M)/\langle F_q(M)\rangle_v, \tag{13}$$

that is,

$$C_{p,q}(M) = \left\langle \Phi_q^p(M)\right\rangle_v, \tag{14}$$

which is a double moment introduced earlier for the study of chaotic behavior of particle production in branching processes [35]. Whereas q must be an integer, p need not be. In fact, the derivative of $C_{p,q}(M)$ at $p = 1$, that is,

$$\Sigma_q(M) = \frac{d}{dp} C_{p,q}(M)\bigg|_{p=1} = \langle \Phi_q \ln \Phi_q\rangle_v, \tag{15}$$

has been related to an entropy defined in the event space [35], but by itself it is not very useful because it depends on M.

Simplification can occur if $C_{p,q}(M)$ has a power-law behavior in M,

$$C_{p,q}(M) \propto M^{\psi_q(p)}. \tag{16}$$

Then an (entropy) index can be defined as

$$\mu_q^{(1)} = \frac{d\Sigma_q(M)}{d\ln M} = \frac{d}{dp}\psi_q(p)\Big|_{p=1}, \tag{17}$$

which is independent of M. It was found that $\mu_q^{(1)}$ can characterize the fluctuations of spatial patterns so well that they are as useful as the Lyapunov exponents in providing a quantitative measure of classical chaos [36].

The power-law behavior of $C_{p,q}(M)$ in Eq. (16) has been referred to as erraticity [37,38]. It was proposed as the next logical step to take beyond the intermittency analysis. Attempts have been made to find experimentally the erratic fluctuations of F_q^e from event to event in multiparticle production [17]. In meson-proton collisions at 250 GeV/c beam momentum, it was found that the erracticity measures are dominated by statistical fluctuations at that energy [39]. In nucleus-nucleus collisions interesting signals have been found both in models [40] and in emulsion experiments [41] even at lower energies. The entropy index has also been determined from data on C-Cu collisions at 4.5 A GeV/c, suggesting chaotic behavior in particle production [42]. In Pb-Pb collisions at LHC where we can examine the deconfinement-to-confinement transition, it becomes clear in the next section, where model calculations can generate concrete local multiplicity fluctuations, that it is more comprehensive to consider the range $1 \leqslant p \leqslant 2$ in the study of $C_{p,q}(M)$. If in that range $\psi_q(p)$ has a linear dependence on p, it is better to define the slope in that wider range as

$$\mu_q = d\psi_q(p)/dp. \tag{18}$$

It is this quantity μ_q, referred to as erraticity indices, that will become an effective measure of the criticality classes that is independent of p and M. A large value of μ_q means that there are influential contributions to $C_{p,q}(M)$ from large $F_q^e(M)$ weighted more heavily at large p, which in turn implies that very erratic fluctuations of the spatial patterns are involved to render $F_q^e(M)$ nonvanishing at large q and M.

V. RESULTS OF MODEL CALCULATIONS

We have simulated in the order of 10^6 events for the four models ranging from critical to noncritical cases described in Sec. III. To give visual images of their qualitative differences, we select one event from each case to illustrate their behaviors in the lego plots. For an event to contribute to F_q at $q \geqslant 2$, it cannot be typical if the average bin multiplicity $\langle n\rangle$ is small. We show untypical events that have large n in some bins and thus can contribute to non-trivial F_3 at $M = 30$ and $\Delta p_T = 0.1$ around $p_T = 1$ GeV/c, for which $\langle n\rangle$ is approximately 0.1. In Fig. 2 the four lego plots are arranged as a matrix in the classification given in Table I. Each of the plots corresponds to an event in a given class that contribute to the largest value of $F_3(M)$ at $M = 30$; thus, there should be at least one bin that has a bin multiplicity $n \geqslant 3$. It is evident that the

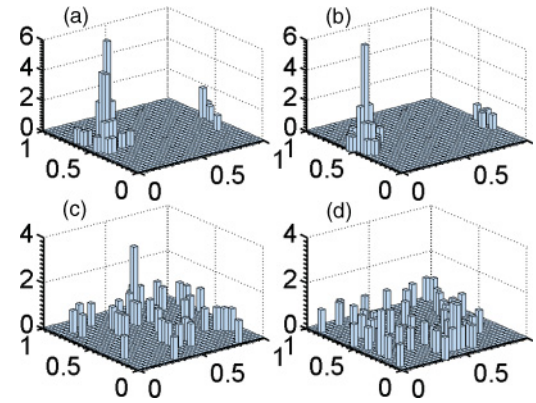

FIG. 2. (Color online) Examples of bin multiplicity fluctuations in (η, ϕ) for the four cases arranged in the matrix form of Table I, that is, (a) critical, (b) quasicritical, (c) pseudocritical, (d) noncritical.

distinctive difference among them is that the pseudocritical and noncritical cases in the lower panels (c) and (d) have particles distributed more widely throughout the base square than in the other two cases above in (a) and (b), where a localized cluster surrounds a high peak. The intent of this figure is only to give a sense of the qualitative difference in the nature of spatial patterns when a stringent demand is placed on the bin multiplicity to depart from the average.

To see the scaling behavior, we examine the vertical averages $\langle F_q(M)\rangle_v$ vs M in log-log plots for $q = 2, \ldots, 5$ and for the cut $\Delta p_T = 0.1$ GeV/c. Hereafter the subscript v is omitted for brevity. For the critical case the results are shown in Fig. 3, where in (a) there is an increase with M before M gets larger than 20, but they all have similar behavior for different q, so when $\langle F_q\rangle$ is plotted against $\langle F_2\rangle$, we see in (b) a simple straight-line behavior for $q = 3, 4, 5$. Using Eqs. (5) and (6) to describe the power β_q, we find in (c) that $\nu_{\rm crit} = 1.41$. Similar properties are found in the quasicritical case with $\nu_{\rm quasi} = 1.33$, as shown in Fig. 4. In the pseudocritical cases, shown in Fig. 5, we see robust scaling behavior in (a). F-scaling behavior in (b) yields the value $\nu_{\rm pseudo} = 1.26$ shown in panel (c). Finally, in the nonscaling case we find the opposite situation where $\langle F_q(M)\rangle$ decreases with increasing

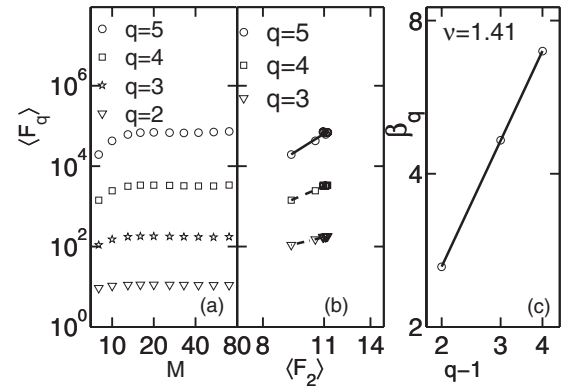

FIG. 3. Intermittency analysis for the critical case. Panels are the same as in Fig. 1.

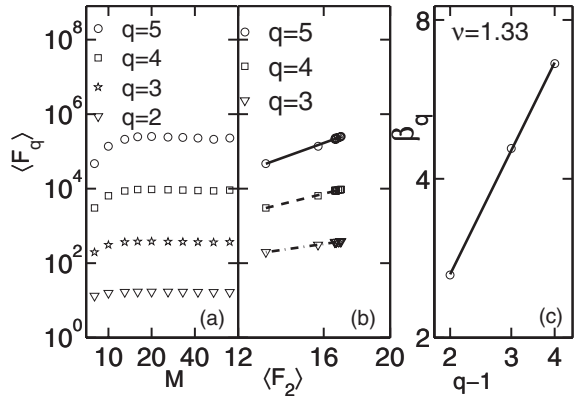

FIG. 4. Intermittency analysis for the quasicritical case. Panels are the same as in Fig. 3.

M, as exhibited in Fig. 6(a). It means that bin multiplicities do not get large enough deviations from $\langle n\rangle$ through random fluctuations so that, when the bin size gets small, $\langle F_q(M)\rangle$ approaches 1 that one expects from Poissonian fluctuations, as stated just below Eq. (4). In (b) we still see regularity in $\langle F_q\rangle$ plotted against $\langle F_2\rangle$, but it is important to recognize that the low end corresponds to high M with all $\langle F_q\rangle$ around 1, while the high end is for low M, quite contrary to the three cases in Figs. 3–5. One can extract the values of $\beta(q)$ as in (c), but there is no sensible value of ν to be assigned to this case. In short, the noncritical case does not yield any interesting result from the study of this kind. We have to go beyond simple intermittency analysis to find a suitable description that can render quantitative comparison between the critical and noncritical cases.

Although the results shown in Figs. 3–5 are clear and easily quantifiable in terms of ν, a great deal of information is lost by calculating those averages. To exhibit the degree of fluctuations of the spatial patterns from the average, let us use $P(\Phi_q)$ to denote the probability distribution of event $\Phi_q(M)$ at fixed M, where $\Phi_q(M)$ is defined in Eq. (13). In Fig. 7 we show $P(\Phi_q)$ for $q = 2$ and 4, and for clarity only for $M = 8$ and 30. The four classes of criticality are again in the matrix format of Table I. We see that in all cases the distributions for $q = 2$ and $M = 8$ (solid lines) are peaked at $\Phi_q = 1$. However, for other values

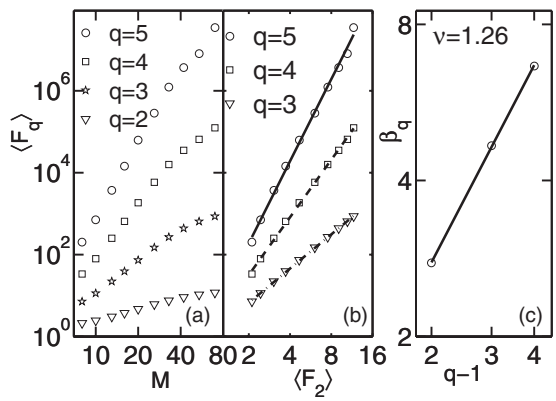

FIG. 5. Intermittency analysis for the pseudocritical case. Panels are the same as in Fig. 3.

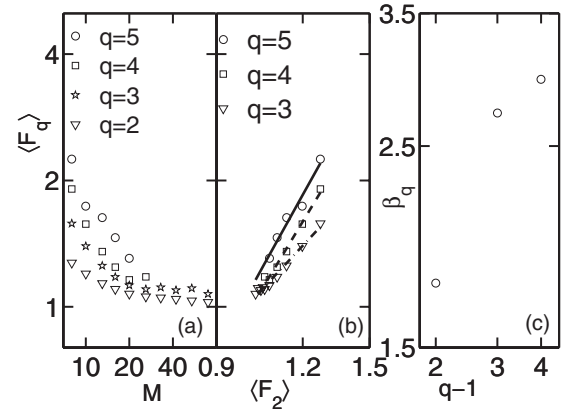

FIG. 6. Intermittency analysis for the noncritical case. Panels are the same as in Fig. 3.

of q and M, the four cases differ in different ways. In the other extreme situation corresponding to $q = 4$ and $M = 30$ (lines with crosses), we see that $P(\Phi_4)$ is peaked at $\Phi_4 = 0$ in all cases. That is because in small bins the average bin multiplicity $\langle n\rangle$ is much less than 4, so the values of Φ_4 for many events are 0. In fact, for (c) pseudocritcial and (d) noncritical, only a small fraction of events have large enough bin fluctuations to render F_4^e nonzero, so $P(\Phi_4)$ has a δ function peak at $\Phi_4 = 0$, whose positions are shifted in Fig. 7 for visibility's sake. In the intermediary values of $q = 4$, $M = 8$, the dashed lines in all four cases are all very broad, signifying wide fluctuations. For $q = 2$, $M = 30$ (dash-dotted lines) the peaks are around $\Phi_2 = 1$, similar to the solid lines.

In the insets of Figs. 7(c) and 7(d) we show that for $q = 4$ and $M = 30$ there are contributions to $P(\Phi_4)$ at extremely large Φ_4 (in the order of 10^3). The vertical axes have the scale factor 10^{-6}. They balance the δ functions at $\Phi_4 = 0$ so that the average is $\langle\Phi_4\rangle_v = 1$, by definition. This irregular behavior reveals the nature of fluctuations from event to event. When the average bin multiplicity $\langle n\rangle$ is about 0.03, it is difficult to find events in which there is a bin with $n \geqslant 4$, unless there

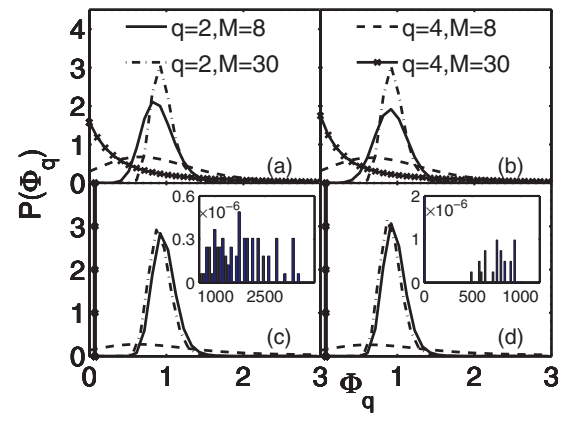

FIG. 7. (Color online) Probability distributions of $\Phi_q(M)$ for various values of q and M. The panels correspond to the criticality cases expressed in Table I and as shown in Fig. 2. The insets in (c) and (d) are for large values of Φ_q as explained in the text. The vertical axes have a common scale factor of 10^{-6}.

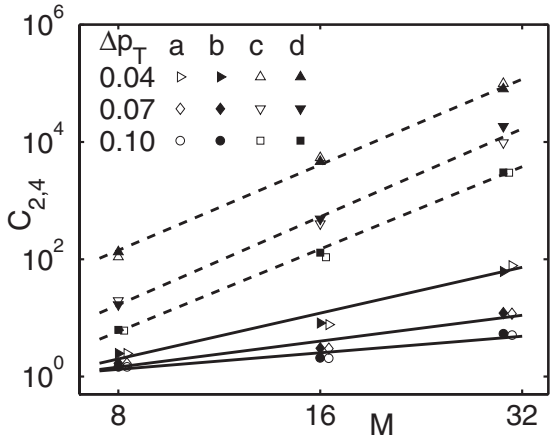

FIG. 8. Power-law behavior of $C_{2,4}(M)$ exhibiting erraticity. The labels a, b, c, d correspond to the four panels in Figs. 2 and 7 in the matrix format of Table I. Pairs of symbols are approximated by one straight line, so 12 types of symbols are represented by 6 lines. Δp_T are in the units of GeV/c and are around the value $p_T = 1$ GeV/c.

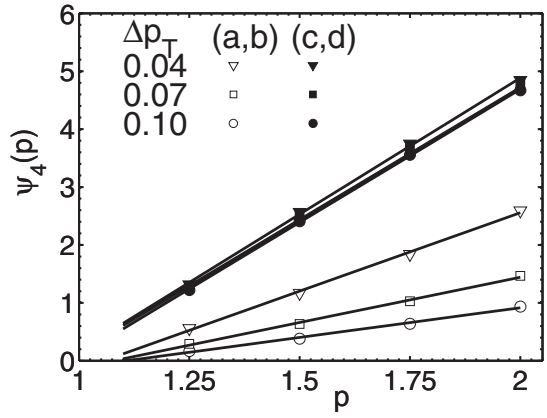

FIG. 9. Linear dependencies of the erraticity exponents $\psi_4(p)$ on p for the (a,b) cases in open symbols and for the (c,d) cases in the solid symbols. Their slopes give the values of the indices μ_4. The units of Δp_T are in GeV/c.

are dynamical effects (such as confinement contraction) to introduce large fluctuations. In cases (c) and (d) almost all events have $n < 4$ so $\Phi_4 = 0$, except for some very rare events that make nontrivial contribution to nonzero Φ_4, whose values are therefore very large because $F_4(M = 30)$ is exceedingly large (owing to the smallness of f_1^4), even though Φ_4 is normalized by $\langle F_4(M = 30)\rangle$, which is proportional to the rarity of such events.

The probability distributions $P(\Phi_q)$ contain too much information that cannot easily be conveyed. We learn from Fig. 7 that for $q = 2$ there are no drastic differences among the four cases when M is increased from 8 to 30. It means that bin multiplicities in each case can fluctuate sufficiently to exceed $n = 2$ and generate a modest width of the peaks in $P(\Phi_2)$ around $\Phi_2 = 1$. We therefore should not expect a good measure at $q = 2$ to distinguish the criticality classes. For $q = 4$, however, we see significant differences between the cases (a) and (b) with contraction and (c) and (d) without contraction. To quantify their differences we consider the moments $C_{p,q}(M)$ defined in Eq. (14). For $p = 2, q = 4$, we show in Fig. 8 the M dependence for three intervals of Δp_T : 0.04, 0.07, and 0.1 GeV/c. The cases a, b, c, and d in the legend correspond to the panels in Fig. 7 arranged in the matrix form of Table I. Some of the open symbols are displaced slightly from $M = 8$, 16, and 30 to avoid them from being covered by the solid symbols. We see that they satisfy power-law behavior very well in all cases, validating the meaningfulness of the erraticity exponents $\psi_q(p)$ defined in Eq. (16). Similar study can be done for $p = 1.25$, 1.5, and 1.75, and yield similar scaling behavior, which we do not show for brevity.

The values of $\psi_4(p)$ are shown in Fig. 9. In that figure the cases (a) and (b) are depicted collectively by open symbols, while the cases (c) and (d) are depicted by filled symbols. The values of $\psi_4(p)$ in the (c,d) group are all larger than those in the (a,b) group. Evidently, there are good linear dependencies on p between 1.25 and 2 in all cases. The straight lines drawn through them are extended only to $p = 1.1$. At $p = 1$ it is necessary that $\psi_q(1) = 0$ because $C_{1,q}(M) = 1$ for any q and M. The lines, if extrapolated further to $p = 1$, would all miss the origin (1, 0) by little bits. There is some reason for that to happen at the point $p = 1$, which we discuss below. For now, we concentrate on the linear portion in Fig. 9 and determine the slopes μ_4, as defined in Eq. (18). It is clear that the (c,d) group has essentially no dependence on Δp_T. Even in the (a,b) group the spread owing to different Δp_T cuts is not severe enough to make it unreasonable for us to give the three lines in each group an average slope as follows:

$$\mu_4^{a,b} = 1.87 \pm 0.84, \qquad \mu_4^{c,d} = 4.65 \pm 0.06. \tag{19}$$

It is remarkable that we can obtain numerical summary of the different cases independent of p and M and only mildly dependent on Δp_T. The values of these indices mean that for the models (a,b) that have contraction owing to confinement there are spikes in bin multiplicity locally, making them easier to have bins with $n \geqslant 4$ (thus lower values of μ_4 or less erratic) than for the models (c,d) that have no contraction. In the latter cases there are not enough multiplicity fluctuations to have $n \geqslant 4$ in most bins and in most events, so the probability of having a nonzero F_4 at high M is extremely low, but in those rare events the value of F_4 is so high (thus more erratic) that the pth moment with $p \geqslant 1.25$ gives them such a high weight as to raise $\psi_4(p)$ and μ_4 significantly above those for (a,b) cases.

Turning now to the complication at the point $p = 1$, we note that if the straight lines in Fig. 9 go through the origin (1, 0) exactly, then the slopes are constant throughout $1 \leqslant p \leqslant 2$ and we could alternatively focus on the point $p = 1$ exclusively. In that case we could return to Eqs. (15) and (17) and determine $\mu_4^{(1)}$ directly from $\Sigma_4(M)$. Unfortunately, we have found that $\Sigma_4(M)$ does not depend on $\ell n M$ linearly, so we are unable to make use of Eq. (17) to calculate the slope at $p = 1$. This is consistent with the fact that the straight lines in Fig. 9 do not cross the origin precisely and that some bending of those lines near the point (1, 0) reveals the lack of universality of the slopes for all p. Stated differently, the power-law behavior of Eq. (16) is not true for all p; the local multiplicity fluctuations

can be so severe and are so different among the four cases that the indices $\mu_q^{(1)}$ at $p = 1$ cannot summarize their differences.

Returning to the results expressed in Eq. (19), we can conclude that what separates (a,b) from (c,d) is the dominating effect of contraction over clustering. Recall from Table I that the two columns are for cases where initial and reseeded configurations between time steps are with clustering (a,c) and without clustering (b,d), while the two rows are for cases where the configurations between time steps undergo contraction (a,b) and no contraction (c,d). Because there are ten substeps within each time step, contractions rearrange the configurations sufficiently so that the erraticity moments $C_{p,q}$ retain essentially no memory of the clustering effects in the input. Physically, it means that as the QGP approaches low density near the end of its expansion, whether or not there is critical clustering, the confinement forces that act on the quarks near the surface exert the dominant effect on drawing the $q\bar{q}$ pairs together to pionize, despite the opposing tendency to randomize owing to thermal activities that persist. The same process is repeated each time a new layer moves to the surface. The tension between confinement and deconfinement is what leads to large local fluctuations evidenced by the low values of the erraticity indices $\mu_4^{a,b}$. Without that tension the bin-multiplicity fluctuations have no dynamical push beyond randomness, so it is highly erratic to have some rare events to contribute to nontrivial $C_{p,4}$, hence higher values of $\mu_4^{c,d}$.

VI. CONCLUSION

The purpose of this work is mainly to describe an unconventional method to analyze the LHC data in the hope that some experimentalists may find it venturesome. The new frontier opened up by the high multiplicity events provides a fertile ground for exploration that is not feasible at lower energies. That is why the subject is not among those predictions that could be extrapolated from RHIC. If there is any hint of critical behavior in the quark-hadron transition, that would be a new discovery at LHC. Even if nothing critical is found, analysis along the line suggested here should lead to deeper understanding of the hadronization process.

When the LHC data are analyzed, how would one know whether something new has been discovered, if there is nothing at RHIC that can be compared to? That is why we have investigated different possibilities in this paper and constructed a framework in which to interpret future LHC results. We have considered four classes of quark-hadron transitions and calculated the erraticity indices μ_4 for each. Those indices are pure numbers, independent of bin number M, order of moments p, and (approximate) size of Δp_T cut. If the LHC data can be analyzed to yield definitive values of μ_4, then it is possible to interpret the result in terms of the criticality discussed here. If the values fall outside the range that we have obtained, it may be even more interesting, because it suggests that our models of the four classes of criticality are unrealistic. In that case a new field of study is then opened up in the face of the experimental values of μ_4.

However, the basic issue is, of course, whether the proposed measures can be applied to the real data to uncover interesting physics. There exist other physical processes that are totally ignored in this study. Chief among them is minijet production, which is understood to be copious in Pb-Pb collisions at 2.76 TeV [43]. Usual jet study at LHC is for p_T very large, for example, >50 GeV/c. Our analysis here is for $p_T \approx 1$ GeV/c, which is minute compared to the jet towers, but the result can nevertheless be affected by thermal-shower recombination. It is unlikely that the low p_T enhancement by minijets can lead to multiplicities greater than 4 in very small bins, but rare events with large fluctuations are what the erraticity moments $C_{p,q}(M)$ are sensitive to. Thus, at this point we cannot rule out contamination of the PT effects by minijets. Such possibilities perhaps would encourage the experimentalists to investigate the subject, either to find resolution of ambiguities or to gain new perspective on an aspect of physics that is not well understood.

ACKNOWLEDGMENTS

We are grateful to Edward Sarkisyan for his interest in this work and his enlightening suggestions. This work was supported, in part, by the US Department of Energy under Grant No. DE-FG02-96ER40972, the National Natural Science Foundation of China under Grant No. 11075061, and the Program of Introducing Talents of Discipline to Universities under Grant No. B08033.

[1] M. Bleicher, J. Phys. G: Nucl. Part. Phys. **38**, 124035 (2011).
[2] B. Mohanty, Nucl. Phys. A **830**, 899c (2009); J. Phys. G: Nucl. Part. Phys. **38**, 124023 (2011).
[3] For reviews, see F. Antinori, J. Phys. G: Nucl. Part. Phys. **38**, 124038 (2011); J. Schukraft (ALICE Collaboration), *ibid.* **38**, 124003 (2011); P. Steinberg (ATLAS Collaboration), *ibid.* **38**, 124004 (2011).
[4] N. Armesto, in *Quark-Gluon Plasma 4*, edited by R. C. Hwa and X. N. Wang (World Scientific, Singapore, 2010), p. 375.
[5] E. K. G. Sarkisyan and A. S. Sakharov, Eur. Phys. J. C **70**, 533 (2010).
[6] K. Aamodt *et al.* (ALICE Collaboration), Phys. Rev. Lett. **105**, 252301 (2010).
[7] G. Aad *et al.* (ATLAS Collaboration), Phys. Lett. B **710**, 363 (2012).
[8] S. Chatrchyan *et al.* (CMS Collaboration), J. High Energy Phys. 08 (2011) 141.
[9] H. Appelshäuser (ALICE Collaboration), J. Phys. G: Nucl. Part. Phys. **38**, 124014 (2011).
[10] F. Cooper and G. Frye, Phys. Rev. D **10**, 186 (1974).
[11] M. Stephanov, Prog. Theor. Phys. Suppl. **153**, 139 (2004); J. Phys. G: Nucl. Part. Phys. **38**, 124147 (2011).
[12] S. Heckel (ALICE Collaboration), J. Phys. G: Nucl. Part. Phys. **38**, 124095 (2011).
[13] P. Christakoglou (ALICE Collaboration), arXiv:1111.4506.
[14] S. Gavin and G. Moschelli, Phys. Rev. C **85**, 014905 (2012).

[15] J. J. Binney, N. J. Dowrick, A. J. Fisher, and M. E. J. Newman, *The Theory of Critical Phenomena* (Clarendon, Oxford, 1992).
[16] A. Bialas and R. Peschanski, Nucl. Phys. B **273**, 703 (1986); **308**, 857 (1988).
[17] W. Kittel and E. A. De Wolf, *Soft Multihadron Dynamics* (World Scientific, Singapore, 2005), p. 429.
[18] E. K. Sarkisyan, L. K. Gelovani, G. L. Gogiberidze, and G. G. Taran, Phys. Lett. B **347**, 439 (1995).
[19] D. Ghosh *et al*., J. Phys. G: Nucl. Part. Phys. **26**, 405 (2000).
[20] D. Ghosh *et al*., Phys. Rev. C **68**, 024908 (2003); **68**, 027901 (2003); **70**, 054903 (2004).
[21] D. Ghosh *et al*., J. Phys. G: Nucl. Part. Phys. **31**, 1083 (2005).
[22] T. Nakamura (PHENIX Collaboration), Nucl. Phys. A **774**, 627 (2006).
[23] K. Homma (PHENIX Collaboration), POS **CPOD2006**, 007, arXiv:nucl-ex/0703046.
[24] M. Mohsin Khan *et al*., Ind. J. Phys. **85**, 195 (2011).
[25] S. Bhattacharyya, D. Ghosh, and A. Deb, Physica A **390**, 4144 (2011).
[26] A. Bialas and R. C. Hwa, Phys. Lett. B **253**, 436 (1991).
[27] R. C. Hwa and M. T. Nazirov, Phys. Rev. Lett. **69**, 741 (1992); R. C. Hwa, Phys. Rev. D **47**, 2773 (1993).
[28] M. R. Young, Y. Qu, S. Singh, and R. C. Hwa, Opt. Commun. **105**, 325 (1994).
[29] H. Haken, Rev. Mod. Phys. **47**, 67 (1975).
[30] Z. Cao, Y. Gao, and R. C. Hwa, Z. Phys. C **72**, 661 (1996).
[31] R. C. Hwa, C. S. Lam, and J. Pan, Phys. Rev. Lett. **72**, 820 (1994); R. C. Hwa and J. Pan, Phys. Rev. C **50**, 2516 (1994).
[32] R. C. Hwa and C. B. Yang, Phys. Rev. C **67**, 034902 (2003); **70**, 024905 (2004).
[33] V. Greco, C. M. Ko, and P. Lévai, Phys. Rev. Lett. **90**, 202302 (2003); Phys. Rev. C **68**, 034904 (2003).
[34] R. J. Fries, B. Müller, C. Nonaka, and S. A. Bass, Phys. Rev. Lett. **90**, 202303 (2003); Phys. Rev. C **68**, 044902 (2003).
[35] Z. Cao and R. C. Hwa, Phys. Rev. Lett. **75**, 1268 (1995); Phys. Rev. D **53**, 6608 (1996).
[36] Z. Cao and R. C. Hwa, Phys. Rev. E **56**, 326 (1997).
[37] R. C. Hwa, Acta Phys. Pol. B **27**, 1789 (1996).
[38] Z. Cao and R. C. Hwa, Phys. Rev. D **61**, 074011 (2000).
[39] M. R. Atayan *et al*. (EHS/NA22 Collaboration), Phys. Lett. B **558**, 22 (2003).
[40] F. M. Liu, H. Liao, M. Liu, F. Liu, and L. S. Liu, Phys. Lett. B **516**, 293 (2001).
[41] D. Ghosh, A. Deb, M. Mondal, and J. Ghosh, Phys. Lett. B **540**, 52 (2002).
[42] L. K. Gelovani, G. L. Gogiberidze, and E. K. Sarkisyan, in *Correlations and Fluctuations '98*, Proceedings of the 8th International Workshop on Multiparticle Production, edited by T. Csörgö, S. Hegyi, G. Jancsó, and R. C. Hwa (World Scientific, Singapore, 1999), p. 498.
[43] R. C. Hwa and L. Zhu, Phys. Rev. C **84**, 064914 (2011).